

LBL--28838

DE90 011604

Presented at the 6th Winter Workshop on Nuclear Dynamics,
Jackson Hole, Wyoming U.S.A., 17-24 February 1990.

**Collision Dynamics and Particle Production
in Relativistic Nucleus-Nucleus Collisions at CERN**

John W. Harris
Nuclear Science Division, Lawrence Berkeley Laboratory,
University of California, Berkeley, CA 94720, USA
and the
NA35 Collaboration

DISCLAIMER

This report was prepared as an account of work sponsored by an agency of the United States Government. Neither the United States Government nor any agency thereof, nor any of their employees, makes any warranty, express or implied, or assumes any legal liability or responsibility for the accuracy, completeness, or usefulness of any information, apparatus, product, or process disclosed, or represents that its use would not infringe privately owned rights. Reference herein to any specific commercial product, process, or service by trade name, trademark, manufacturer, or otherwise does not necessarily constitute or imply its endorsement, recommendation, or favoring by the United States Government or any agency thereof. The views and opinions of authors expressed herein do not necessarily state or reflect those of the United States Government or any agency thereof.

This work was supported by the Director, Office of Energy Research, Division of Nuclear Physics of the Office of High Energy and Nuclear Physics of the U.S. Department of Energy under Contract DE-AC03-76SF00098

MASTER M
DISTRIBUTION OF THIS DOCUMENT IS UNLIMITED

Collision Dynamics and Particle Production in Relativistic Nucleus-Nucleus Collisions at CERN

John W. Harris

Nuclear Science Division, Lawrence Berkeley Laboratory,

University of California, Berkeley, CA 94720, USA

and the

NA35 Collaboration

1. Introduction

The possibility of forming a quark-gluon plasma is the primary motivation for studying nucleus-nucleus collisions at very high energies. Various "signatures" for the existence of a quark-gluon plasma in these collisions have been proposed. These include an enhancement in the production of strange particles,¹ suppression of J/Ψ production,² observation of direct photons from the plasma,³ event-by-event fluctuations in the rapidity distributions of produced particles,⁴ and various other observables. However, the system will evolve dynamically from a pure plasma or mixed phase (of plasma and hadronic matter) through expansion, cooling, hadronization and freezeout into the final state particles. Therefore, to be able to determine that a new, transient state of matter has been formed it will be necessary to understand the space-time evolution of the collision process and the microscopic structure of hadronic interactions, at the level of quarks and gluons, at high temperatures and densities. In this talk I will review briefly the present state of our understanding of the dynamics of these collisions and, in addition, present a few recent results on particle production from the NA35 experiment at CERN.

2. Collision Dynamics

2.1 Geometry

Information on the geometry of nucleus-nucleus collisions can be obtained from measured interaction cross sections, multiplicity distributions, rapidity distributions and the distributions of energy in the transverse and longitudinal directions in an event. The interaction cross sections are found to have a geometrical dependence on the radii of the colliding nuclei and are observed to be independent of incident energy for energies from 2 GeV/n to 200 GeV/n.^{5,6} The transverse energy distributions are observed to be impact parameter dependent and support a "clean-cut" geometrical overlap of the colliding nuclei.^{7,8} For the nucleus-nucleus case of A_P projectile nucleons incident on A_T target nucleons the transverse energy distributions can be reproduced by an A_P -fold convolution of proton-nucleus (A_T) collisions over the same range of impact parameters.^{7,8} The first and second moments of multiplicity distributions for nucleus-nucleus collisions are well described by a superposition of proton-nucleus collisions,⁵ rather than a superposition of pp collisions. The rapidity distributions of produced particles have been measured and are observed to peak at the rapidity of the center-of-mass of the geometrical overlap of the colliding nuclei.⁹ This information provides support for the important role that geometry plays in the dynamics of these collisions.

2.2 Freezeout Characteristics

Hanbury Brown and Twiss (HBT) correlations¹⁰ between negative pions have been measured for various systems by the NA35 Collaboration. The approach involves a Gaussian parameterization¹¹ of the pion-emitting source, at the time when interactions cease (freezeout), with R_T the transverse radius, R_L the longitudinal radius and Λ the chaoticity parameter. Another parameterization¹² of the source distribution which is Lorentz-covariant and incorporates the inside-outside cascade for the collision dynamics determines the parameters R_T , Λ and the source lifetime τ_0 . A value of $\Lambda = 1$ corresponds to chaotic emission from the source. Values of $\Lambda < 1$ correspond to decreasing chaoticity, with $\Lambda = 0$ total coherence. In 200 GeV/n O + Au reactions, pions at $2 < y < 3$ near midrapidity in the effective $^{16}\text{O} + \text{Au}$ center-of-mass ($y_{cm} = 2.5$) originate from a large ($R_T \simeq 8$ fm), relatively chaotic ($\Lambda \simeq 0.8$), long-lived ($\tau_0 = 6.4$ fm/c) source.¹³

This picture suggests the formation of a thermalized fireball at midrapidity. Considering the large number of produced particles, mostly pions, near midrapidity in central collisions of O + Au at 200 GeV/n (approximately 120 - 140 per unit rapidity^{9,13}) and the $\pi\pi$ strong interaction cross sections, one predicts a similar size ($R \simeq 8$ fm) for a thermalized system of pions at freeze-out. Preliminary NA35 results on HBT correlations for negatively-charged pions from central 200 GeV/n S + Ag and S + Au collisions exhibit this same effect, a large source of midrapidity pions. Examining these data as a function of the pion multiplicity of the event it is found that for pions at midrapidity the source radius increases with the multiplicity. For the lighter S + S system at midrapidity and for the heavy target systems away from midrapidity the transverse size is near that of the incident projectile, the longitudinal size is smaller and the chaoticity parameter is low similar to that observed in HBT measurements in e^+e^- and hadron-hadron collisions.

2.3 Thermalization and Nuclear Stopping

As stated in section 2.1, the locations of the peak positions of the rapidity distributions of produced particles are consistent with a simple geometrical overlap picture of the collision process. The distributions are Gaussian in shape and are broader than expected for emission from an isotropic fireball. Whether the rapidity distributions represent a large degree of stopping in the Landau¹⁴ sense or partial stopping as predicted by string mechanisms in the Lund/FRITIOF model¹⁵ is still undetermined. Up to now, the Landau and string models both predict the measured rapidity distributions of produced particles at CERN energies. The talk by Prakash in this Workshop addresses the subject of the proper use of the Landau model and how its results compare to the data.

Rapidity distributions of protons are not yet available from experiment for nucleus-nucleus collisions at CERN. The NA35 Collaboration has measured rapidity distributions of "charge flow", which can be associated with protons, by subtracting all negative from positive particles to obtain the "protons" displayed in Fig. 1. Also shown are the rapidity distributions of negative particles and Λ 's, both of which peak at midrapidity. These data are for 200 GeV/n S + S central reactions. Also displayed for comparison are the negative particle rapidity distribution for 200 GeV p + p

minimum bias data, arbitrarily normalized to be able to compare to the S + S data. The S + S data are reflected about $y = y_{cm} = 3$. The rapidity distributions for negative particles from the minimum bias p + p and central S + S reactions are nearly identical in shape, suggesting the same production mechanism with little or no rescattering in the two cases. The rapidity distributions of "protons" from the S + S reaction is spread out in rapidity and exhibits significantly more stopping than predicted in the Lund/FRITIOF model which underpredicts the "proton" yield at $y = y_{cm} = 3$. Another string model VENUS 2¹⁶ has been successful in predicting the "proton" rapidity distribution using breakup of leading diquarks.

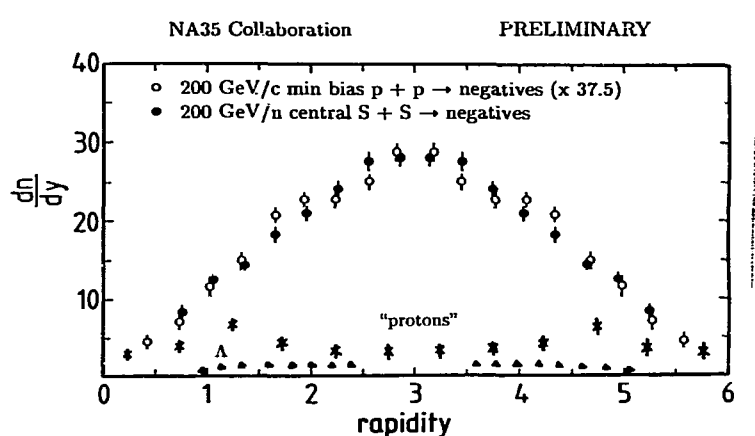


Fig.1. Rapidity distributions of negative particles, "protons" and Λ particles for central collisions of 200 GeV/n S + S and negative particles for minimum bias collisions of 200 GeV/c p + p (arbitrarily normalized for comparison). The data are reflected about $y = y_{cm} = 3$.

The degree of nuclear stopping and details of the energy densities reached in nucleus-nucleus collisions at CERN energies, both derived from transverse energy distributions, are described in the talk of Plasil in this Workshop.

3. Particle Production

3.1 Strange Particle Production

The NA35 Collaboration has measured the production of strange particles in 60 and 200 GeV/n p + Au and O + Au and in 200 GeV/n S + S collisions.^{17,18} Displayed in Fig. 2 is the mean number of Λ particles per event as a function of the mean charged particle multiplicity of the events for S + S reactions. The Λ production increases with centrality of the collision at a rate faster than that predicted by the Lund/FRITIOF model and faster than a superposition model of nucleon-nucleon

data. The same dependence is also observed for $\bar{\Lambda}$ and K^0 production. For central collisions the Λ yield is more than a factor of two larger than predicted by any of the models, including a hadron gas model, with the exception of a parton gas model. For details of the models and comparisons see Ref. 19. The ratios of $\langle \Lambda \rangle / \langle \pi^- \rangle$, $\langle \bar{\Lambda} \rangle / \langle \pi^- \rangle$ and $\langle K^0 \rangle / \langle \pi^- \rangle$ also increase with centrality of the collision. These enhanced strange particle production yields have yet to be explained in terms of simple nuclear phenomena.

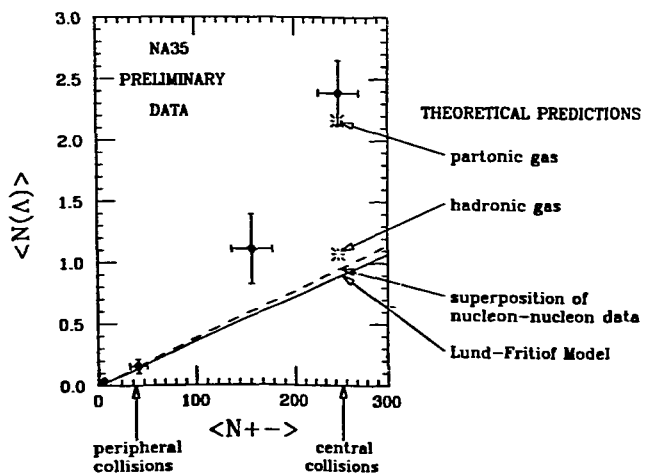


Fig.2. The mean multiplicity of Λ particles as a function of the mean charged particle multiplicity for 200 GeV/n S + S collisions. See text for model descriptions.

3.2 Transverse Mass and Momentum Distributions

The transverse momentum distributions of produced particles have the potential of providing information on the freezeout temperature, hydrodynamical flow effects and possibly the primordial, critical temperature of the system prior to expansion and freezeout. In the absence of flow effects the lower p_\perp part of the spectrum should reflect the freezeout conditions. However, flow effects would distort this part of the spectrum and these effects might be identified in the p_\perp distributions for various detected particle types and systems. Displayed in Fig. 3 are transverse mass (m_\perp) distributions, where $m_\perp = (p_\perp^2 + m^2)^{1/2}$, of various particles at midrapidity for central collisions of 200 GeV/n O + Au and S + S. Plotted are $m_\perp^{-3/2} dn/dm_\perp$ as a function of m_\perp . Using relativistic thermodynamics as developed by Hagedorn²⁰ for a single isotropic fireball, a Boltzmann distribution after integration over rapidity gives $dn/dm_\perp = \text{constant } m_\perp^{3/2} e^{-m_\perp/T}$ for large m_\perp/T . Thus $m_\perp^{-3/2} dn/dm_\perp$ plotted as a function of m_\perp should be a negative exponential for large enough m_\perp . This appears to be the case for the measured Λ , K^0 and "proton" distributions as well as the large m_\perp end of the π^- spectra. The straight lines correspond to $dn/dm_\perp = \text{constant } m^{3/2}$

$e^{-m_T/T}$ with $T = 200$ MeV. Is this the critical transition temperature?

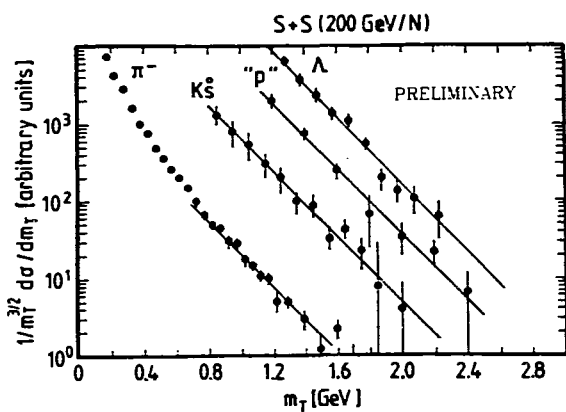
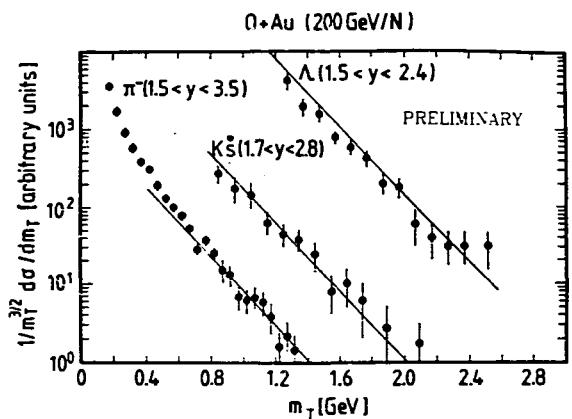


Fig.3. Transverse mass distributions for various particles in central collisions of 200 GeV/n a) $\Omega + \text{Au}$ and b) $S + S$. The rapidity intervals for a) are on the figure while those for b) are $0.8 < y < 2.0$, $1.5 < y < 3.0$, $1.4 < y < 2.7$ and $1.5 < y < 3.5$ for Λ , p , K^0 and π^- , respectively. The straight lines correspond to a temperature of 200 MeV in the Hagedorn fireball model.

The measured m_\perp distributions of pions are generally nonthermal in shape and may be a complicated mixture of the effects of freezeout, flow and possibly a critical temperature. Using the velocity of sound in an ultrarelativistic gas, $c/\sqrt{3}$, we can estimate the m_\perp regime where hydrodynamic flow will have a large effect. Hydrodynamic flow would have its greatest effect in the lowest m_\perp part of the spectrum where $m_\perp < 1.22$ m. Recent analysis²¹ of this data and that for π^0 production from WA80 in a radial flow model concludes that the spectra can be fit with an average radial flow velocity of approximately $c/2$ and a freezeout temperature of 100 MeV. The initial temperature in this model before expansion is 200 MeV, similar to that derived from the high m_\perp part of the particle spectra of Fig. 3. Another analysis of the measured pion p_\perp distributions in terms of hydrodynamical flow appears in the talk of Ruuskanen in this Workshop.

4. Acknowledgements

This work was supported by the Director, Office of Energy Research, Division of Nuclear Physics of the Office of High Energy and Nuclear Physics of the U.S. Department of Energy under contract DE-AC03-76SF00098.

References

1. R. Hagedorn and J. Rafelski, Phys. Lett. 97B (1980) 180.
2. T. Matsui and H. Satz, Phys. Lett. B178 (1986) 416.
3. L.D. McLerran and T. Toimela, Phys. Rev. D31 (1985) 545.
4. L. Van Hove, Z. Phys. C27 (1985) 135.
5. A. Bamberger et al., Phys. Lett. B205 (1988) 583.
6. P. Barnes et al., Phys. Lett. B206 (1988) 146.
7. A. Bamberger et al., Phys. Lett. B184 (1987) 271.
8. L.P. Remsberg et al., Z. Phys. C38 (1988) 35 and W. Heck et al., Z. Phys. C38 (1988) 19.
9. H. Ströbélé et al., Z. Phys. C38 (1988) 89.
10. R. Hanbury Brown and R.Q. Twiss, Nature 177 (1956) 27 and Nature 178 (1956) 1046.
11. F.B. Yano and S.E. Koonin, Phys. Lett. B78 (1978) 556.
12. K. Kolehmainen and M. Gyulassy, Phys. Lett. B180 (1986) 203.
13. A. Bamberger et al., Phys. Lett. B203 (1988) 320.
14. L.D. Landau, Collected Papers, No. 88, Izv. Akad. Nauk, Ser. Fiz. 17 (1953) 51.
15. B. Andersson et al., Nucl. Phys. B281 (1987) 289.
16. K. Werner, BNL Preprint BNL-42 435 (1989).
17. A. Bamberger et al., Z. Phys. C43 (1989) 25.
18. J. Bartke et al., U. Frankfurt Preprint (1990).
19. M. Gazdzicki et al., Nucl. Phys. A498 (1989) 375c.
20. R. Hagedorn, CERN 71-12 (1971); GSI-Report 81-6 (1981) 236;
Proceedings of Quark Matter 84, ed. K. Kajantie, Springer-Verlag (1985) 53.
21. K.S. Lee and U. Heinz, Z. Phys. C43 (1989) 425.